Assessment of the Pore Diameter Measured in Gas-Liquid Displacement Porometry: Effect of the Capillary Constant

Ängeslevä Marina, Salmimies Riina, Rideal Graham, Häkkinen Antti

Assessment of the pore diameter measured in gas-liquid displacement porometry: effect of the capillary constant

M. Ängeslevä[1*], R. Salmimies[1], G. Rideal[2†], A. Häkkinen[1]

[1]LUT School of Engineering Science, Lappeenranta – Lahti University of Technology LUT,

P.O. Box 20, FI-53851 Lappeenranta, Finland

[2†]Whitehouse Scientific Ltd, Whitchurch Road, Waverton, Chester CH3 7PB, UK.

*Corresponding author: Tel.: +358 40 221 2652, email: marina.angesleva@gmail.com,

https://orcid.org/0000-0002-4717-6455

ABSTRACT

Determining pore sizes of porous media accurately is essential for many reasons. The standard ASTM F316 describing calculations used in gas-liquid displacement (GLD) porometry includes a factor B or a capillary constant. The standard does not explain the nature of this factor and the reasons for using its value. This work aimed to investigate the capillary constant, to understand its meaning and applicability in calculating the pore diameter. Another goal was to assess the pore diameter measured in GLD porometry by comparing it with pore diameters measured with image analysis and cut point test methods. Seven filter media samples with as simple a structure as possible were analyzed. An investigation of the capillary constant revealed at least five different approaches, of which all are by no means applied for the calculations of pore size. Using the

approach described in standard ASTM F316 to adjust the values obtained by GLD porometry was found unsuitable for the simply structured samples studied in this work. This work showed that the pore diameters measured by GLD porometry were most comparable with the other studied techniques when using Silwick as the wetting liquid. The raw data of bubble point pore and mean flow pore diameters measured by GLD porometry were similar to the largest pore sizes and mean pore diameters measured by image analysis and cut point test methods. This, in turn, confirmed the absence of the need to use any constants for calculating the pore diameters for the samples studied in this work.

1. Introduction

Porous materials, such as textiles, ceramics, metals, membranes, and polymers, are widely used as filter media. Defining structural parameters of these materials, such as pore size, pore size distribution, porosity, pore shape, and pore tortuosity, is vital in developing, designing, and selecting porous materials for separation processes (Belov, 1987; Jena and Gupta, 2010; AlMarzooqi et al., 2016; Yu et al., 2010).

One of the most widely used techniques for measuring pore diameters and pore size distributions is gas-liquid displacement (GLD) porometry (Islam et al., 2020). This technique is also called capillary flow porometry or wetting liquid extrusion flow porometry (Gupta, 2010). The method involves saturating a porous material with a wetting liquid and forcing inert gas through the pores. This procedure includes a series of pressure steps resulting in displacing the wetting liquid by the gas. The porometer equipment controls the gas flow rate and the resulting pressure difference is measured. Based on the measurement of pressure and the corresponding volumetric flow rate of gas passing through the pores, the pore diameter, and the pore size distribution are calculated (Kolb et al., 2018; ASTM F316-03, 2011; Maalal et al., 2022).

GLD porometry has many advantages. The tests performed according to this technique are non-destructive, i.e., the filter medium remains unchanged after completion of the test (Rushton et al., 2000). This works only when the wetting liquid is completely removed from the pores during the measurement. The technique allows measuring the largest and mean pore size, pore size distribution (PSD), pore size range, gas permeability and envelope surface area (Gupta, 2010).

On the other hand, GLD porometry is often criticized by the scientific community. The main criticism is that the technique assumes that the pore space consists of a bundle of non-intersecting

pores or parallel cylindrical capillary tubes of a circular cross-section. However, this is a gross oversimplification since the structure of most real porous materials is way more complicated. The porous materials consist of interconnected and non-interconnected pores, dead-end pores, pores with irregular cross-section, etc. (Maalal et al., 2021a; Maalal et al., 2022; Mourhatch et al., 2011; Morison, 2008; Scheidegger, 1963). Mourhatch et al. (2011) have demonstrated that the simple representation of the porous media as a bundle of non-intersecting pores leads to erroneous PSDs that are much narrower than the real ones. Similar results were reported by Maalal et al. (2022). Maalal et al. (2021a) also pointed out that the technique is not able to differentiate between throats (constrictions in the pore space) and pore bodies (local larger cavities). Islam et al. (2020) concluded that the law governing gas flow through capillaries under the conditions of porometry data acquisition are not well-formulated. Since the porometer avoids using a flux equation, very little information is obtained about the pore uniformity or tortuosity, and no information is provided about the number of pores corresponding to a specific pore range. Mourhatch et al. (2011) reported that the correct interpretation and utilization of data for determining the PSD is a challenging task and, in some sense, a separate issue.

Indeed, the determination and calculation of PSD includes many nuances and parameters that should be carefully studied to substantiate the interpretation of data correctly and scientifically. Currently, not all the necessary parameters used by the standard ASTM F316-03 (2011) describing the GLD technique are explained and clarified. For example, the capillary constant included in calculating the pore diameter remains obscure. The standard does not define the capillary constant, does not provide a physical meaning of it, and does not explain the need for its use in calculations. Like any other parameter included in the equation for calculating the pore diameter, the capillary

constant dramatically influences the final result. Therefore, this parameter deserves particular attention and should be investigated and explained.

According to Gupta (2010), the pore diameter measured in GLD porometry is calculated by the Young-Laplace equation:

$$d = \frac{4\sigma \cos\theta}{\Delta P} \tag{1}$$

where d is the pore diameter (m), σ – surface tension of the liquid (N/m), θ is the contact angle between the surface of the porous material and the liquid, ΔP is the applied pressure necessary to empty the pores filled with the wetting liquid. In the case of complete wetting of the porous material by the liquid, the contact angle is assumed to be zero (ASTM F316-03, 2011; Kikoin and Kikoin, 1976).

The Young-Laplace equation describes the shape of the liquid interface or meniscus inside the pore at equilibrium, i.e., when the pressures on both sides of the air/wetting liquid interface are equal. The meniscus is formed only in sufficiently narrow tubes, i.e., at low Bond number ($B_0 \ll 1$). The latter is calculated as follows:

$$B_o = \frac{\Delta \rho g R^2}{\sigma} \tag{2}$$

where B_0 is the Bond number (-), $\Delta\rho$ is the density difference between two fluids namely gas and wetting liquid (kg/m^3), g is gravitational acceleration (N/kg), R is the radius (m), σ is the surface tension or the interfacial tension between two gas and wetting liquid (N/m) (Jin et al., 2020). Most equipment employing GLD porometry are based on and meet the conditions described in the standard ASTM F316 (2011). The standard is fundamental because it describes the main principles of porometry and includes all the equations and graphs used in the technique. According to the

standard ASTM F316 (2011), equation 1 is modified to include a capillary constant B that is claimed to be equal to 0.715:

$$d = \frac{4\sigma B cos\theta}{\Delta P}$$

(3)

The symbol B is used for the capillary constant in all equations in this manuscript to signify the same parameter, even though the symbol for the capillary constant varies in the literature.

The user manual for the PMI Capillary Flow Porometer (CFP-1500AEXCS, 2009) also states that the software of this equipment uses the same constant in the calculation of the pore diameter. In contrast, the book (Gupta, 2010), written by the developers of this equipment, describes the calculation of the pore diameter without using any constants. An independent calculation of the raw data obtained with the PMI Capillary Flow Porometer was carried out by the authors of this article. The results of this procedure showed no additional constants used in the calculations. This contradiction must be resolved, and the question arises whether any constant should be used when calculating the pore diameter measured by GLD porometry. Therefore, one of the main goals of this paper was to study and understand the concept of the capillary constant, to which the standard and the manual referred. This paper attempted to evaluate the need to use the capillary constant to calculate the pore diameter in GLD porometry. Additionally, the quality of the pore diameter measured by GLD was assessed by comparing it with the pore diameters measured by the image analysis and cut point tests methods.

The presented paper addressed the issues by summarizing different theories of the capillary constant, performing tests with the capillary flow porometer, and validating the obtained results by comparing them with the pore diameters measured by two other techniques. Thus, 1) a literature review regarding the capillary constant was carried out, and all possible concepts of the capillary

constant found by the authors were described; 2) the pore diameters of different samples were measured by PMI Advanced Capillary Flow Porometer; 3) the measured results were compared with the pore diameters obtained by the image analysis and cut point tests; 4) comparative analysis of pore diameters obtained by using three different techniques were done. Based on the obtained information, the quality of the pore diameters measured by porometry was assessed. This analysis, in turn, revealed the necessity of using the capillary constant to calculate the pore diameter in GLD porometry.

2. Theoretical foundations of the capillary constant

According to the standard ASTM F316 (2011), the equation for calculating the pore diameter is derived from the determination of the surface tension of a liquid. As mentioned above, the standard does not explain the capillary constant, its physical meaning, or units of measurement. When looking at the existing literature, it quickly becomes apparent that there are different definitions of the capillary constant. For example, the definition of a "capillary constant" can be found in the description of an experimental "maximum bubble pressure" method to determine the surface tension of a liquid (Frolov, 1988; Savitskaya and Shimanovich, 2003). The method is similar to GLD porometry except that the capillary is submerged in the wetting liquid, and the capillary radius is already known. Inert gas is pushed through the wetted capillary under continuously increasing pressure. Maximum gas pressure is reached when the bubble becomes a sphere, and the radius of the bubble equals the radius of the capillary. The experimental dynamic-surface-tension curves obtained by this method depend on the apparatus constant (Christov et al., 2006), which some (Frolov, 1988; Savitskaya and Shimanovich, 2003) also referred to as a capillary constant. A standard liquid with known surface tension can be used to determine the capillary constant (by a calibration procedure) and to avoid an error in measuring the curvature of the meniscus (or the

radius of the capillary). Knowing the surface tension of the liquid, a capillary constant is calculated using the equation (Frolov, 1988):

$$\sigma = B\Delta P \tag{4}$$

The equation is also used to calculate the surface tension of other liquids from experimental data. B in this equation stands for the capillary radius (Rcap/2) from a general equation used to calculate the surface tension by the maximum bubble pressure method (Miller and Fainerman, 2001). The capillary constant in equation 4 does not depend on the nature of the wetting liquid, its concentration, or a bubbling period, but it has different values for apparatuses of different constructions and depends on the gas supply system (Christov et al., 2006; Frolov, 1988; Savitskaya and Shimanovich, 2003). The capillary constant here has a constant value for a single capillary used for the measurement of surface tension and can be calculated by the equation:

$$\frac{r_k \rho g}{2} = B = \frac{\sigma_k}{\Delta h^k{}_{max}} \tag{5}$$

where r_k is the radius of the known and used capillary (m), σ_k is the surface tension of the known and used liquid (N/m) and $\Delta h^k{}_{max}$ is the maximum height of the fluid in the capillary (m) (Savitskaya and Shimanovich, 2003). The apparatus constant can also be determined by analyzing video recordings of the bubbling process to draw a conclusion about the bubble point. The experimentally derived value of B is further used for quantitative interpretation of data obtained with the same apparatus to determine surface tension (Christov et al., 2006).

The capillary constant can also be used to characterize a system in which capillary phenomena become significant. The capillary constant describes the maximum pore diameter, where the equilibrium forms between surface tension and gravity. In other words, if a liquid upon entering a tube forms a meniscus, capillary phenomena are considered relevant in this tube, and the tube is

deemed a capillary. The use of a capillary constant in such a manner makes it possible to distinguish between capillaries and pipes (tubes). If the diameter of a tube is equal to or smaller than the capillary constant, the tube can be deemed a capillary. When the diameter is significantly larger than the capillary constant, the capillary forces are insignificant, and the tube is considered a pipe. The capillary constant as described in this way is between 1 – 3 mm for most liquids. For example, the capillary constant of water at 20º C is equal to 3.8 mm and can be calculated by the equation:

$$B = \sqrt{\frac{\sigma}{g(\rho_l - \rho_g)}} \tag{6}$$

where ρ_l and ρ_g are the densities of the liquid and the gas within the capillary, respectively, and B is the liquid-specific capillary constant (m) (Labuntcov and Yagov, 2007; Mayer, 2008; Richards and Carver, 1921). The capillary constant can sometimes be expressed through the capillary radius, too (Kashin et al., 2011):

$$\frac{2\sigma}{\rho g} = rh = B^2 \tag{7}$$

where r is the radius of the capillary (m). Kashin et al. (2011) noted that equation 7 is incorrect due to uncertainties related to the interpretation of the liquid height. The liquid height, h, can be defined as the height up to the bottom of the meniscus or up to the maximum height of the liquid at the pore walls. Different researchers, thus, can interpret the height differently, ending up with differing capillary constants. Kashin et al. (2011) suggested calculating the capillary constant using a strictly defined volume of a liquid in the capillary:

$$\frac{\sigma}{\rho g} = \frac{V}{l} = B^2 \tag{8}$$

where V is the volume of liquid in the capillary (m³), and l is the wetting perimeter of the capillary walls at the point of meniscus formation (m).

Some researchers (Hutten, 2016; Hernandez et al., 1996; Siau et al., 1981) have noted that the standard ASTM F316 originates from a method presented by Bechhold (1908). This method includes overcoming the surface tension, as well as the measurement of permeability at different pressures. The pore diameter and the pore size distribution are calculated from the pressure required to blow air through a porous membrane wetted with water. Hutten (2016) describes that Bechhold developed a capillary constant B, which is included in the standard ASTM F316 and is equal to 0.715 and that this constant is actually a tortuosity factor. Bechhold (1908) used the following equation for the calculation of the pore diameter:

$$d = i \frac{4B}{p \cdot 1.033 \cdot 10^5} \tag{9}$$

where p is the atmospheric pressure (atm.), i is a factor influencing fluid flow through a filter (-), B is a capillary constant of water having a value of 7.7 at 18 ° C (Bechhold, 1908). The factor i was assigned values from 0.1 to 1.0, but no range was reported for the capillary constant. The reasoning behind choosing 0.715 for the ASTM F316 standard is not discussed within the standard (ASTM F316-03, 2011). Zhang et al. (2010) have also concluded that the capillary constant is a tortuosity factor, which can be derived from equation:

$$l = Bl_o \tag{10}$$

where l is the actual length of the capillary (m), l_o is the apparent length of the capillary (m). Al-hadidi (2011) assigned the capillary constant as "the change in the size (pore diameter) along the pore."

Jena and Gupta (2010) and AlMarzooqi et al. (2016) propose that the value of 0.715 in the ASTM F316 standard is a pore shape factor. Jena and Gupta (2010) say that many pores are characterized by an elliptical cross-sectional shape. The shape factor for an elliptical pore is 0.72. The shape factor B can be calculated by the equation:

$$B = \frac{d}{D} \tag{11}$$

where B is a shape factor (-), d is the diameter of the largest particle that can pass through the elliptical pore (m), and D is the pore diameter measured by capillary flow porometry (m) (Jena and Gupta, 2010; AlMarzooqi et al., 2016). Herper (2017) paid particular attention to the capillary constant when calculating the pore diameter for wire meshes. He mentioned that the value of the capillary constant B, which was used in the standard ASTM F316 and equal to 0.715, is a correction factor, which "includes all deviations from a perfect cylinder shape" and was only valid for one specific pore geometry. He emphasized that it is crucial to calculate the capillary constant, or a capillary correction factor, for each weave individually.

All the information described above is summarized in Table 1. As can be seen from the table, there are several interpretations of the meaning of the capillary constant, almost as many units for the capillary constant, and relatively little information on the justification of the use of 0.715 as the capillary constant in the standard ASTM F316. The capillary constant directly affects the reported pore size and pore size distribution in GLD porometry. This paper aims to evaluate the pore diameter data from GLD porometry by comparing the results with some other methods of pore size determination. Furthermore, the use of the capillary constant from standard ASTM F316 is evaluated.

Table 1 Different interpretation of the capillary constant.

	Author	Equation	Interpretation
1	Frolov, Y.G. (1988) Savitskaya, T.A. and Shimanovich, M.P. (2003)	$\sigma = B\Delta P$ $\dfrac{r_k \rho g}{2} = B = \dfrac{\sigma_k}{\Delta h^k{}_{max}}$	B is capillary specific and does not depend on the liquid. B has units of kg/ms².
2	Labuntcov, D.A. and Yagov, V. V. (2007) Mayer, V. V. (2008) Richards, T.W. and Carver, E.K. (1921) Kashin, V.V. et al. (2011)	$B = \sqrt{\dfrac{\sigma}{g(\rho_l - \rho_g)}}$ $\dfrac{2\sigma}{\rho g} = rh = B^2$ $\dfrac{\sigma}{\rho g} = \dfrac{V}{l} = B^2$	B is liquid specific only. It is equal to $1 - 3$ **mm** for most liquids and describes the maximum pore diameter where capillary forces are relevant for that specific liquid.
3	Hutten, I. M. (2016) Hernandez, A. et al. (1996) Siau, J. F. et al. (1981) Zhang, H. et al. (2010) Al-hadidi, A.M.M. (2011)	$B = \dfrac{l}{l_o}$	B is a dimensionless tortuosity factor.
4	Jena, A. and Gupta, K. (2010) AlMarzooqi, F.A. et al. (2016)	$B = \dfrac{d}{D}$	A value **0.715** used in Capillary Flow Porometry as a capillary constant B is represented in some references as a shape factor. The shape factor for elliptical pores is 0.72.
5	Herper, D. (2017)	$\Delta P = \dfrac{4\sigma B}{d}$	B is a dimensionless correction factor that describes

			all deviations from a perfect cylindrical shape and has an individual value for each weave type.

3. Materials and methods

3.1. Materials

To study the influence of the capillary constant on the calculation of the pore diameter, an attempt was made to minimize the effects of tortuosity and pore shape by selecting appropriate samples. Firstly, samples with a square pore cross-section were chosen. According to Gupta (2010), the shape factor of pores with this cross-section is equal to 1. Secondly, one layer meshes were selected to minimize the effect of tortuosity, i.e., samples with a tortuosity of 1, or close to 1, were selected. Thirdly, the samples were chosen with as simple a porous structure as possible to resemble the pore space consisting of a bundle of non-intersecting pores. According to a simple model presented by Green et al. (2008), a fabric can be described as a material consisting of pores, which resemble tubes in parallel having a common inlet and outlet.

The studied samples were electroformed sieves produced by Gilson Company, Inc. and weave meshes manufactured by Asada Mesh Co., Ltd. Three electroformed sieves were analyzed: Gilson 15.8, Gilson 20.7, and Gilson 25.5, with the number indicating the nominal pore size in micrometers. All the Gilson samples were made from nickel. In turn, four weave meshes – Asada 16, Asada 34, Asada 45, and Asada 55, again the number indicating the nominal pore size – were analyzed. The Asada samples were made of 316 Stainless Steel. No information on the method of

determination of the nominal pore size was provided by the manufacturers. The information about structural characteristics of the studied samples, such as the weave pattern, count of cloth, thickness and wire diameters, and open area, are presented in Table 2. Microscope images of the samples are shown in Fig. 1.

Table 2   Characteristics of filter media samples

Sample name	Weave pattern	Count of cloth, End density/ Pick density	Thickness [µm]	Wire diameters [µm]	Open area [%]
Asada 16	2/2 twill	15 x 795	37.2	15.5	20.8
Asada 34	2/2 twill	30 x 400	61.8	27.8	28.1
Asada 45	2/2 twill	32 x 330	85.5	33.3	33.3
Asada 55	plain	23 x 325	54	22.2	47.5
Gilson 15.8	EF	-	40	-	4.9
Gilson 20.7	EF	-	24.7	-	16.0
Gilson 25.5	EF	-	36	-	16.0

3.2. Pore size measurement

To evaluate the accuracy of the pore diameter and study the presence of the capillary constant in the calculations carried out by the PMI equipment, BPPD and MFPD were compared with the pore diameters obtained via image analysis and cut point tests. Although all these techniques measured the pore diameter, the measurement process and data representation differed. The pore diameter measured indirectly by GLD porometry provided the hydraulic pore diameter. In contrast, direct measurement methods, such as the cut point test and microscope analysis, provided the value of the relevant pore diameter of the largest sphere, which could pass through the pore. This diameter can also be called geometric pore size or an equivalent pore size (the largest circle inserted in the pore). To compare the pore diameters directly and indirectly measured, a sample should consist of pores whose relevant pore diameter correlates with the hydraulic diameter.

Anlauf (2016) conducted a comparative analysis of direct and indirect techniques for measuring the pore diameter. To compare the hydraulic pore diameter (d_{equ}) with the relevant pore diameter of the largest sphere (d_{max}), the researcher evaluated the conversion factor (k), which allowed to calculate d_{max} from the measured d_{equ}. The approach to determine k was based on formulating a force balance vertical to the pore cross-section. Anlauf (2016) found that based on the force balance inside the pore with the square cross-section, the equivalent pore diameter and maximal diameter of the sphere corresponded to the side length of the square. In this case, the conversion factor was equal to 1, i.e., d_{max} was equal to d_{equ}, and the bubble point diameter was identical to the geometrical pore size. The researcher validated this conclusion by experiments with edged sieves and monofilament fabrics.

In this work, single-layer monofilament samples and electroformed sieves with throughgoing pores having square cross-sections were chosen to perform the comparison. Based on Anlauf's (2016) conclusions, the hydraulic pore diameter measured by the PMI equipment is equal to the geometric pore size measured by image analysis and cut point test for such samples. Therefore, the comparison of these techniques was possible to perform in this work. The description of the techniques is presented in the following chapters.

3.2.1. Capillary Flow Porometry

The PMI Advanced Capillary Flow Porometer was used to measure the pore size of the samples. A brief description of the method used by this equipment was described in the introduction.

Before the initial testing, the sample was wetted under a vacuum for half an hour to fill the pores of the samples with the wetting liquid and remove any air bubbles from inside the pores. In this work, three different wetting liquids were used: reverse osmosis purified water (surface tension is 0.0728 N/m at 20º C), Galwick with the chemical name propene, 1,1,2,3,3,3 – hexafluoro (surface tension is 0.0159 N/m), and Silwick or silicone oil (surface tension for Silwick is 0.0201 N/m). The manufacturer did not provide information about the temperature at which the surface tension for these wetting liquids had been determined. PMI Inc. was the provider of the last two liquids. The densities of the wetting liquids were measured by a pycnometer. They were 998.21 kg/m^3 for water, 1795.1 kg/m^3 for Galwick, and 935.01 kg/m^3 for Silwick at 20 ºC. Liquids with distinctly different characteristics were selected to investigate the effect of the liquid on the capillary constant, as some theories claim the capillary constant to be dependent on the wetting liquid (Labuntcov and Yagov, 2007; Mayer, 2008; Richards and Carver, 1921; Kashin et al., 2011).In a typical experiment with the PMI equipment, air at a set flow rate is supplied to the sample chamber.

This results in a constant rate of pressure increase, according to the PMI user manual (CFP-1500AEXCS, 2009). The volume flow rate of gas is measured and controlled by a mass flow meter (V2incr), while the pressure valve (preginc) is connected to a pressure transducer and monitored by a computer. The output of the flow transducer to the computer is in counts. The counts are used as units of measure, where 1 count equals 0.1 cc/min. Salmimies (2012) mentioned that the pressure and flow increments and the parameters related to detecting the bubble point (F/PT factor) are highly important. These parameters influence the accuracy of the obtained data and the duration of the tests; therefore, their proper determination is essential. The researcher reported that the pressure and flow increments determine the number of data points in a given pressure range. The minimum number of counts for the flow and pressure increments were chosen based on initial investigations to provide the most accurate results. For the flow regulator, it corresponded to 5 counts, and for the pressure 0.3 counts. The F/PT factor, which is associated with detecting the bubble point pore diameter, was set to 100. This factor determines the moment at which the bubble point pressure is recorded. The bubble flow was set to 2.4 cm^3/min. Adapter plates with the diameter of the circular testing area of 16 mm were used to accommodate the thin samples used in this work. The pressure range was from 0 to 0.05 bar. The tests were performed for all the samples and each test was repeated three times. It should be mentioned that the operator can set a tortuosity factor for the PMI porometer. For this work, the tortuosity factor was set to 1.

The measurement with the porometer is done with a dry and wet sample. The equipment records the flow of gas through a dry sample, and the dry curve, or a plot of flow rates versus the applied pressure, is built. The procedure is repeated on a sample wetted with a wetting liquid, and the wet curve is obtained. The software of the PMI equipment uses the pressure at which wet flow is one-half the dry flow to calculate the mean flow pore diameter (MFPD) using equation 3. The same

17

equation is employed to calculate the bubble point pore diameter (BPPD) using the first pressure step (the PMI user manual CFP-1500AEXCS, 2009). Since the purpose of this paper was to evaluate the quality of pore diameter measured by the PMI equipment, only raw MFPD and BPPDs obtained directly by the device were used for analysis in this work. Independent calculations of BPPD carried out by the authors of this study showed that the device provided diameter values without applying any constants. In addition, the BPPD and MFPD were recalculated for Gilson samples when Galwick was used as a wetting liquid. As will be mentioned in section 3.3., this wetting liquid did not wet these samples completely. The standard deviation (SD) error for MFPDs was within 0.3 - 7.6 %, and 0.1 – 11 % for the BPPDs. In addition, the pore size distribution was not discussed and analyzed in this work. The authors devoted a separate article to investigating the pore size distribution measured and calculated by the PMI equipment.

3.2.2. Image analysis technique

The pore diameter of the samples was also measured by using the PoreSizer[TM]-instrument provided by the Whitehouse Scientific Ltd. PoreSizer[TM] is a static image analysis system consisting of an optical microscope with a zoom lens, a high-resolution camera, and a software system that processes all the collected data. Before each test, a performance check was done to validate the selected calibration and image settings. For this purpose, certified reference standards and a reference graticule from National Physical Laboratory (NPL) were used. After the performance check was done, a sample was placed under the microscope. Objective lenses x5 and x10 were used to obtain the images. A 1.4-megapixel camera captured slide images at 1392 x 1040 pixels. The total number of pores measured and analyzed by the PoreSizer[TM] was around 1000 for each sample. The coefficient of variation (a standardized measure of dispersion defined as the ratio of the standard deviation to the mean value) was within ±1 %. The size of a pore was determined by

measuring the maximum and minimum aperture dimensions (the measurement range of the PoreSizer™ was from 5 to 300 µm). The equipment recorded an average of three measurements in each direction. The thickness of the wires was also measured using the equipment making multiple measurements in X and Y directions. SD error was 0.8 – 6.6 %.

3.2.3. Cut point test

The geometrical pore size of the samples was determined in challenge testing, i.e., using a cut point test. The term "cut point" specifies the boundary size of a spherical particle that a filter medium allows passing. Particles in the feed, whose size is at or above the cut point, are retained on the filter medium, while particles smaller than the cut point pass through the filter medium. The cut point test can be run using a gas or a liquid carrier medium. Both were done in this work.

A liquid carrier is required to transport particles through the filter medium whose pores are below 20 μm. In this case, an aqueous ultrasonic pulsed flow method was used. The filter media with pores above 20 μm were analyzed by a sonic gravimetric test performed on the Gilson sonic auto shifter. Whitehouse Scientific Ltd. provided all the required equipment for the testing.

Before each test, particles of known size were selected. All particles were certified by their diameters using NIST electroformed sieves. After that, the performance check of the instrument, described above, was done: the weight of the particles on a reference mesh was measured on calibrated scales before each test.

In the dry test, intense oscillating air currents fluidized a known weight of dry particles through the filter medium. The particles that passed through the filter medium were collected, and their weight was measured. The cut point was determined using a calibration graph from the weight percentage of the particles passing. In the aqueous test, particles in a water suspension were passed

through the filter medium using a susceptible vacuum pump to accelerate the process. The PoreSizer[TM] image analysis – instrument analyzed the particles that passed through the sample to determine the cut point and the geometrical pore size. SD error was 1.7 – 4 %.

3.3. Contact angle measurement

To calculate the pore diameter by equation (2), the contact angle (*cos θ*) should be determined. This characteristic was measured by Attension Theta Optical Tensiometer (Biolin Scientific AB). In this equipment, a drop of liquid is placed on the surface of the studied material. If the liquid spreads and wets the surface, the surface is called hydrophilic, and the contact angle in the solid-liquid-air interface is smaller than 90°. In contrast, if the liquid drop maintains its form, the surface is called hydrophobic, and the contact angle in the solid-liquid-air interface has values above 90°.

Contact angles were measured using the studied wetting liquids: reverse osmosis purified water, Galwick, and Silwick. A drop volume of 5 µL for water and 1 – 3 µL for the other two liquids was placed on the surfaces of 316 stainless steel and nickel samples with a micro syringe and a pipette. The measurement was performed on the flat, dense surfaces of the same materials used in this study. These sample materials did not contain any pores to influence the contact angle measurement and were chosen to avoid misinterpretation of the results. As Maalal et al. (2021 b) mentioned, when the droplet is placed on a porous surface, interpreting the results obtained with the sessile drop method is far from straightforward. The contact angle was measured on five different points for each sample, and the arithmetic mean of recorded data was used as the final result. The measurements were made at 23° C. Examples of contact angle measurements are shown in section 4.2, Fig. 2.

4. Results and discussion

4.1. Sample characterization

The PoreSizer^{TM} provided microscope images of the samples. Images of all the samples are presented in Fig. 1.
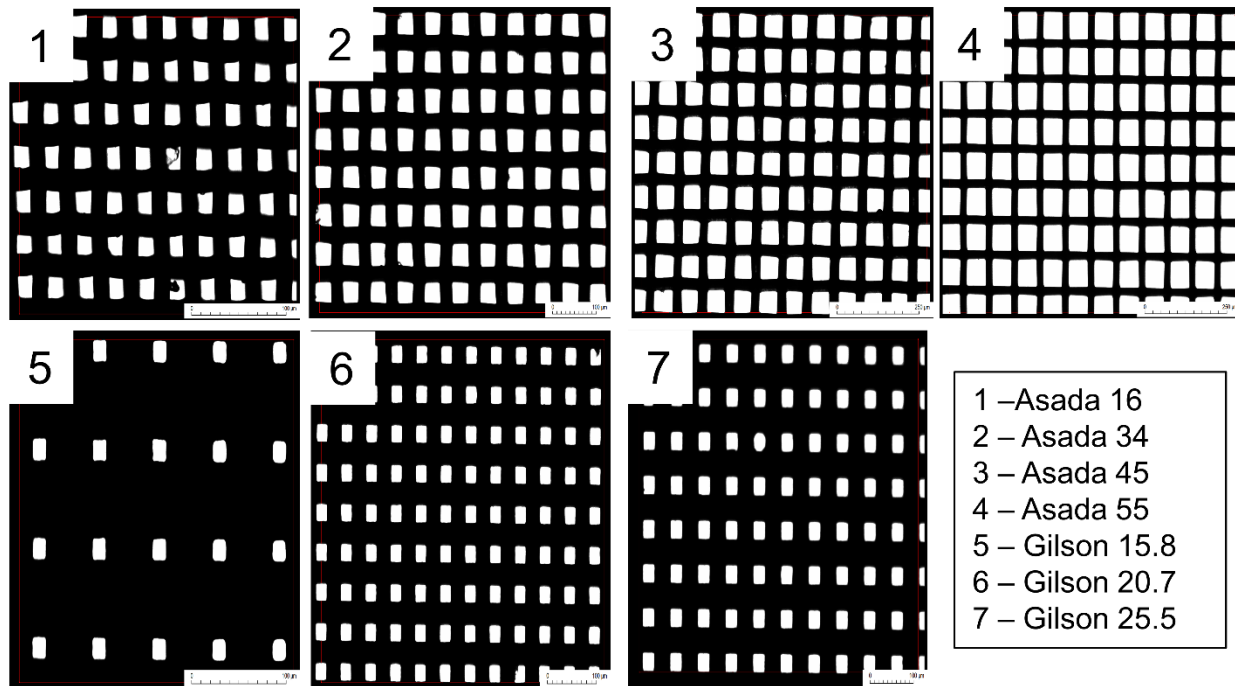

Fig. 1 Sample images taken by PoreSizer^{TM}.

As seen from Fig. 1, all the samples had square-like, relatively homogeneous pores. The square shape was clearer in electroformed sieves (samples 5 (Gilson 15.8), 6 (Gilson 20.7), and 7 (Gilson 25.5). The regularity of the pore shape of electroformed sieves is due to the production method of photo etching and electroforming. Photo etching removes metal from a continuous sheet, while electroforming builds metal layers, depositing it upon a substrate, thus creating a perforated sheet (Purchas and Sutherland, 2002). Asada samples, in turn, were weave meshes made of metal yarns.

Due to the bending of the yarns during the production of woven media, the pores have more variation in their shape than the pores in the electroformed sieves. Although the image analysis provided information only on the shape of the pores (view from above or from x-axis), probably, the pore paths (cross-section or view from y-axis) within the electroformed sieves are less tortuous than in the woven mesh samples due to the different production process.

As shown in Fig. 1, samples 1 (Asada 16), 3 (Asada 34), and 6 (Gilson 20.7) had insignificant but still noticeable deviations inside the pores. All the samples were cleaned thoroughly with ultrasound, meaning that the deviations were integral parts of the samples and not contaminants. Where deviations occur, those naturally reduce the observed pore size affecting the airflow and the measurement results.

4.2. Contact angle results

The contact angle measurement results showed that the reverse osmosis purified water did not wet the studied samples. The contact angle between water and nickel was 102.5 ° and between water and stainless steel 92.2 °, as shown in Fig. 2, indicating low wettability of the samples. The standard deviation with water was 0.9 (stainless steel) and 2.1 % (nickel). These results exclude water as a wetting liquid in GLD porometry for the particular samples studied in this work. PMI manual (CFP-1500AEXCS, 2009) also does not recommend using water or liquids with similar properties to water for testing due to the rapid evaporation of the liquid from the pores of the material being tested. The wetting liquid could evaporate from the pores even before pressure increases sufficiently to force the fluid out. Increasing the pressure is assumed to accelerate the evaporation of the wetting liquid within the pores. According to PMI (CFP-1500AEXCS, 2009), water evaporation is especially significant for very thin and permeable samples, but specifics on

what would qualify as very thin or permeable are not precisely defined. Despite reverse osmosis purified water not being an ideal – or even a good – choice of wetting liquid, in some cases, the use of water is required and could be justified. Salmimies et al. (2012) have selected water as the wetting liquid in studying the regeneration of ceramic filter media because using another wetting liquid easily results in contamination of the samples preventing their further use. Furthermore, if the goal is to evaluate changes in the pore size distribution rather than the absolute pore size, the errors originating from the selection of the wetting liquid might play a less significant role. Nonetheless, the use of water as the wetting liquid would not be advisable if one wants to evaluate the suitability of different methods of pore size determination.
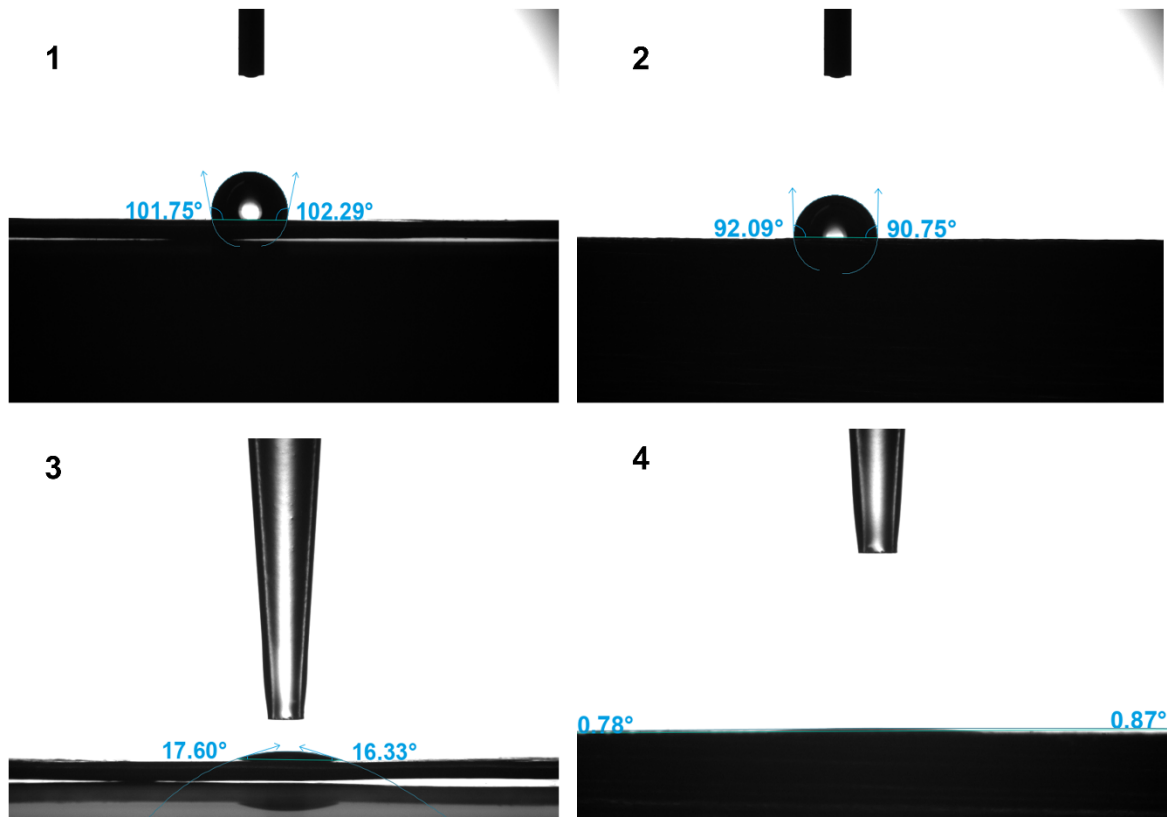
1 – Nickel and water; 2 – Stainless steel and water;
3 – Nickel and Galwick; 4 – Stainless steel and Galwick.

Fig. 2 Contact angle measurements with reverse-osmosis purified water and Galwick on nickel and stainless-steel samples. Here, image 4 was taken after 5 seconds to illustrate the wetting phenomenon (contact angle is slightly higher than 0°). After 6 seconds and beyond, contact angle became 0° leaving no images recorded. With Silwick wetting the material instantaneously, no meaningful images could be recorded.

Galwick thoroughly wetted the stainless steel, i.e., the contact angle was zero (SD was 0 %). The contact angle between this wetting liquid and nickel was 18 ° (SD – 7.2%). This result indicated

that the wettability of this material was also relatively high, though not complete. Silwick thoroughly wetted both test materials, and the contact angles were zero (SD – 0%), respectfully.

4.3. Results of capillary flow porometry

Once the raw results measured by the porometer were obtained (i.e., the volumetric flow rate and the corresponding pressure), the pore diameter was calculated manually using equation 2. The comparison of the manually computed results with the results calculated by the software of the porometer showed that the calculation of the pore diameter by the software was done without the use of 0.715, or a factor *B*.

The pore diameters measured by the porometer using Galwick and Silwick wetting liquids are shown in Table 3, Fig. 3 and 4.

Table 3   The bubble point pore diameter and the mean flow pore diameter measured by capillary flow porometry using Silwick and Galwick. Pore diameter was also measured by the PoreSizer[TM] and the Cut Point test and is presented as D97 and D99.5 (D97 means a pore size below which 97 % of all the pores fall and D99.5 corresponds to a pore size below which 99.5 % of all the pores fall).

Sample	Nominal Size, μm	BPPD[1], μm		MFPD[2], μm		Pore sizer, μm (D97)	Open area, %	Cut point test, μm	
		silwick	galwick	silwick	galwick			Cut point (D97)	Max size (D99.5)
Asada 16	16	16	18.7	14.7	18	16.1	20.8	17.4	18.1
Asada 34	34	34.8	38.5	30	35.4	35.2	28.1	35.2	40.5
Asada 45	45	53.1	58.8	41	52.7	45.9	33.3	46	48.3
Asada 55	55	65.7	95.8	55.7	72.7	54.8	47.5	54.4	56
Gilson 15.8	15.8	12.2	12.4	12	11.6	15.8	4.9	15.1	15.5

Gilson 20.7	20.7	18.3	18.9	17.1	18.6	21.2	16	20.9	21.3
Gilson 25.5	25.5	21.7	23.3	19.8	22.9	26.3	16	25.7	26.3

[1]BPPD – bubble point pore diameter, [2]MFPD – mean flow pore diameter.

As seen from Table 3 and Fig. 3 and 4, the bubble point pore diameter (BPPD) and the mean flow pore diameter (MFPD) of an individual sample differed depending on the wetting liquid and sample material used. According to Fig. 3 and 4, the results obtained with Galwick for Asada samples made of stainless steel were higher than those measured with Silwick even though both wetting liquids wetted the stainless-steel material completely. According to Kolb et al. (2018), the largest source of errors in porometry is the wetting liquid, especially the volatility of the wetting liquid. Authors highlighted that although the vapor pressure of wetting liquids used in the porometry was typically quite low at room temperature, the airflow through the porous samples accelerated the kinetics of the evaporation significantly. The authors concluded that silicone oil, commercially named Silwick, had the lowest rate of evaporation in comparison to other wetting liquids used in porometry. Silwick is not volatile unlike Galwick. Presumably, despite the increasing pressure, Silwick sits inside the pores until the capillary forces are overcome by the external pressure yielding correct results.

Although Galwick wetted the stainless-steel samples completely, the results obtained with this wetting liquid were overestimated for all the Asada samples. As seen in Fig. 3 and 4, higher degree of overestimation correlated with the pore size. The larger the pore size was, the higher the percentage of overestimation was observed. For example, the BPPD measured with the Galwick was 16.9% for Asada 16, 30.6 % for Asada 45, and 74.2 % for Asada 55, higher than the nominal pore size. A similar trend was observed for the MFPDs. Here, the results measured with Galwick were 12.5 % for Asada 16, 17% for Asada 45, and 32% for Asada 55, higher than the nominal pore sizes. Thus, the higher the pore diameter, the higher the surface area that made it easier for the

Galwick to evaporate from such pores. Zhang and Ni (2014) found that both Galwick and Silwick wetting liquids could produce consistent, repeatable, and reliable results of the BPPD. As this study showed, the results obtained with Galwick wetting liquid were overestimated for all the samples used in this study.

The results obtained with Galwick for the Gilson samples were also higher than the nominal pore sizes and those obtained with Silwick. As the contact angle measurement results in the previous section showed, Galwick did not wet the nickel samples completely. The contact angle was 18°. According to the standard ASTM F316 (2011), when the contact angle is greater than zero, the calculated effective pore size will be larger than the actual effective pore size rating. However, when the authors processed these results by applying the contact angle information, they aligned with the results obtained with Silwick, as shown in Fig. 3. The standard, however, stated that the wetting liquid must completely wet the porous samples with the contact angle being zero. Galwick did not wet the nickel material completely. Therefore, it cannot be used as a proper fluid for the analysis of Gilson samples. Moreover, the contact angle between Galwick wetting liquid and the tested material should be analyzed before beginning any tests with the porometer. As the results of this work showed, although the manufacturers described Galwick as liquid that completely wets all surfaces, the wetting might be incomplete depending on the tested material.
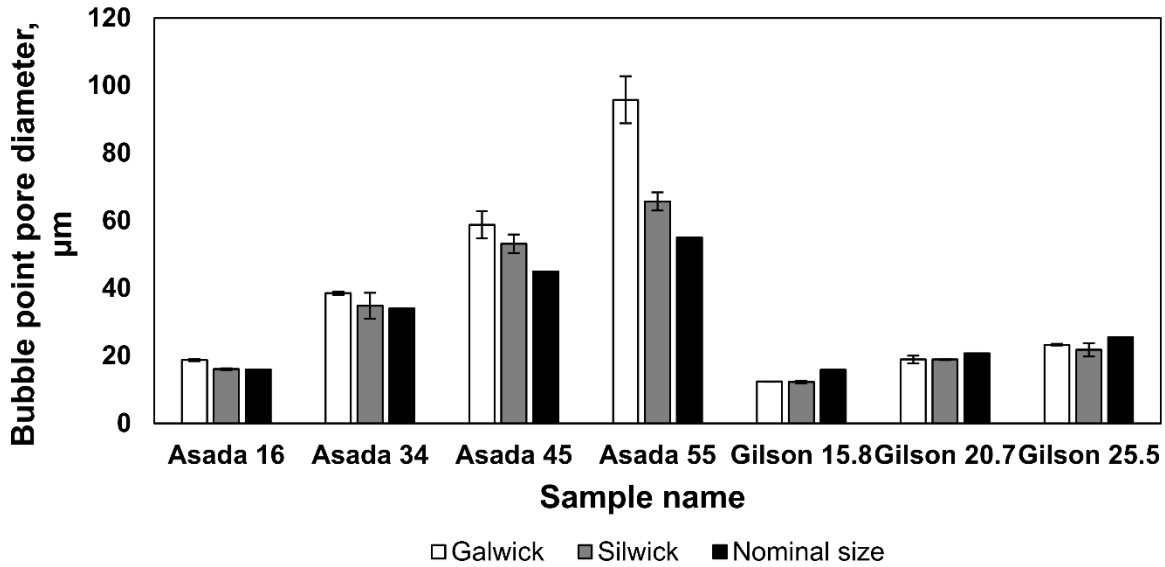
Fig. 3   Bubble point pore diameter measured by capillary flow porometry using Galwick and Silwick wetting liquids. The nominal size was reported by the media manufacturer.

The results with Silwick were, however, much closer to the nominal pore size for most of the samples made of nickel and stainless steel. Moreover, this was the only fluid that wetted the studied materials completely. According to the standard ASTM F316 (2011), the wetting liquid must completely wet the material sample. Thus, in this study, Silwick was the only liquid that satisfied this condition. For materials studied here, Silwick as the wetting liquid best matches most of the nominal pore size. However, it is worth remembering that the nominal pore size is just another pore size measured with another method, as well, and does not necessarily represent the absolute truth any better than any other pore size measurement methods. Except for regularly shaped uniformly sized pores with zero tortuosity, the pore size can be expressed in many ways. Furthermore, in selecting a wetting liquid one should consider whether or not it is vital to remove

the wetting liquid from the sample after the measurement. Silwick is difficult to remove from porous materials and might not always be suitable for the application in mind.
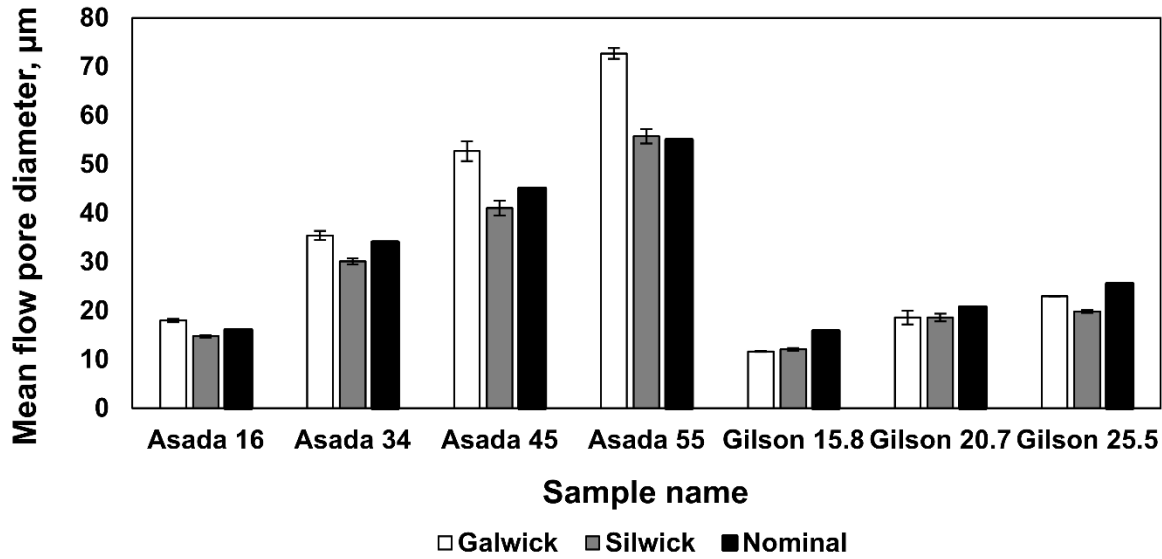

Fig. 4 Mean flow pore diameter measured by capillary flow porometry using Galwick and Silwick wetting liquids. The nominal size was reported by the media manufacturer.

4.4. Comparison of techniques to measure the pore diameter

To assess the quality of the pore diameters measured in porometry, the pore diameters (the BPPD and MFPD) measured by GLD porometry were compared with the pore diameters measured with image analysis and the cut point test. The results of the three techniques are shown in Table 4 and Fig. 5.

Table 4 Comparison of test methods for measuring the pore diameter.

	PMI (silwick)	PoreSizer^{TM}	Sonic Challenger Tester

Sample name	BPPD, μm	Δd, %*	MFPD,	Δd, %*	APD[1],	Δd, %*	Pore size (D97), μm	Δd, %*	Max size (D100), μm	Δd, %*	Median diameter	Δd, %*	Cut point (D97), μm	Δd, %*	Cut point (D99.5), μm	Δd, %*	Median diameter	Δd, %*
Asada 16	16	0	14.7	-8	14.6	-9	16.1	+0.6	18.1	+13.1	14.8	-7.5	17.4	+8.8	18.1	+13.1	14.7	-8.1
Asada 34	34.8	+2.3	30	-12	26.5	-22	35.2	+3.5	38.7	+13.8	33.4	-1.8	35.2	+3.5	40.5	+19.1	29.2	-14.1
Asada 45	53.1	+18	41	-9	31.5	-30	45.9	+2	51.6	+14.7	44.2	-1.8	46	+2.2	48.3	+7.3	41.1	-8.7
Asada 55	65.7	+19.4	55.7	+1.2	43.6	-21	54.8	-0.4	57.4	+4.4	53.5	-2.7	54.4	-1.1	56	+1.8	50.4	-8.4
Gilson 15.8	12.2	-22.8	12	-24	11.9	-6	15.8	0	16.3	+3.2	15.4	-2.5	15.1	-4.4	15.5	-1.9	14.1	-10.8
Gilson 20.7	18.3	-11.6	17.1	-17.4	16.4	-21	21.2	+2.4	21.8	+5.3	21	+1.4	20.9	+1	21.3	+2.9	18.2	-12
Gilson 25.5	21.7	-14.9	19.8	-22.4	17.3	-32	26.3	+3.1	26.7	+4.7	26	+2	25.7	+0.8	26.3	+3.1	22.6	-11.4

[1]APD – Average pore diameter, *the difference between the measured pore diameter and the nominal pore diameter in percentages.

The results for the porometer presented in Table 4 are those measured with Silwick because the comparison of the different wetting liquids showed that Silwick provided the best approximation of the pore size to the nominal pore size and wetted the studied samples completely. The results from the porometer are presented in the form of the BPPD, the MFPD, and the average pore diameter (APD), which was calculated using the arithmetic mean. The geometric pore size measured by the PoreSizer[TM] is expressed as D97, D100, and D50. D97 and D50 represent pore sizes below which 97 % and 50 % of all the pores fall, respectively, and D100 corresponds to the largest pore size in the sample. The cut point results are presented in this work using D97 and D50, comparable to the D97 and D50 measured by the PoreSizer[TM], and as D99.5, which corresponds to a pore size below which 99.5 % of all the pores fall.

D97 and D99.5 were chosen due to the lower measurement uncertainly they provide - only 3 %. According to the wet challenging test results obtained by Rideal and Stewart (2017), using D100

values increases the measurement uncertainty up to 17 %. Therefore, the authors did not recommend using D100 as a reliable parameter. The recommended uncertainty should be less than 5 % for the results to be reliable, as established by the media manufacturer. However, D100 was used in this work to compare with the BPPD obtained in the porometry, because like the BPPD, it represents the largest pore in a sample.
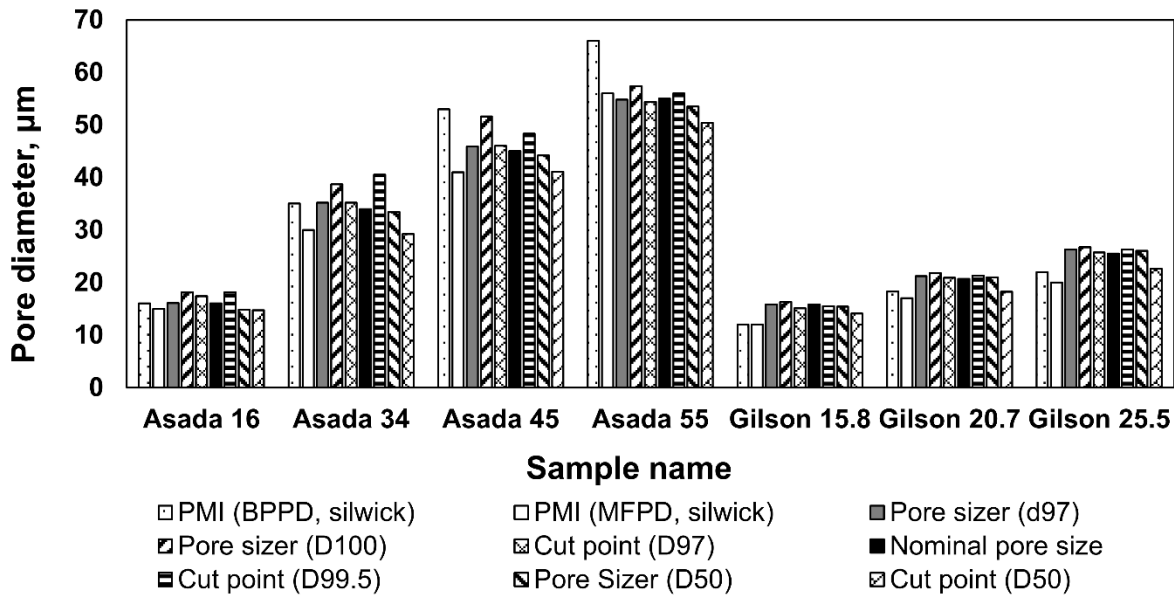

Fig. 5   Comparison of test methods for measuring the pore size. The nominal pore size was reported by the media manufacturer.

As can be seen from Fig. 5 and Table 4, the pore size measured with different techniques was at least for practical purposes in many cases comparable (in the case of MFPD, the pore diameter corresponds to a pore size at which 50 % of the total gas flow through the medium takes place). All the techniques provided deviations to some extent from the nominal pore size for all the studied samples. As mentioned earlier, the media manufacturers did not provide information about the method that was used to determine the nominal pore size. Because detailed information on how the filter media manufacturers determined the nominal pore size was not available, it is difficult to

evaluate how accurate the nominal pore size is and whether it is a good point of comparison for the methods chosen here. Furthermore, it is natural to see differences between different parameters. It is indeed the same parameter measured using different techniques that is interesting.
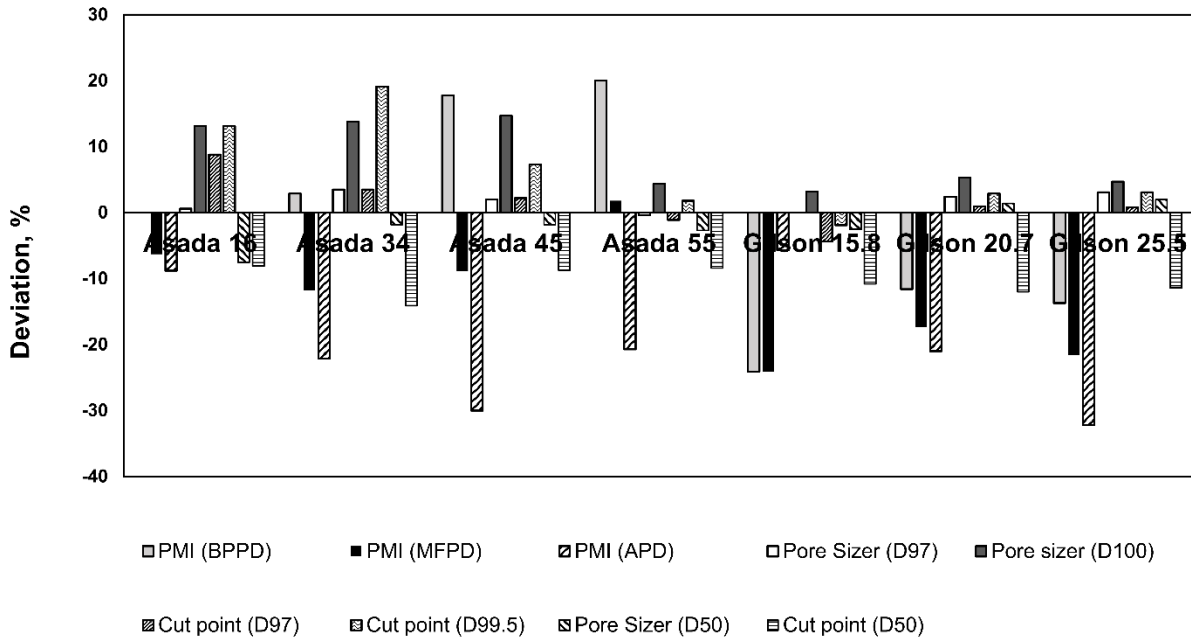

Fig. 6 The deviation of the pore diameter measured by different techniques and the nominal pore size. The nominal size was reported by the media manufacturer.

Fig. 6 demonstrates the relative difference between the measured pore diameter and the nominal pore diameter. The most significant deviations across the board were observed using the APD. APDs are the arithmetic means of the data set obtained through porometry. Based on the information described in Fig. 6 and Table 4, the APD values do not seem to provide comparable results with the nominal pore size as could be expected with pore size distributions not being symmetric. For the data obtained with the PoreSizer[TM], a 2 % omission of outliers, except for Gilson 20.7 and Gilson 25.5, was observed. For commercial purposes, where the goal is to describe

32

the size of the majority of the pores, such data omission can be justified. From a scientific point of view omitting data can result in false conclusions when comparing methods. Especially when averaging or comparing with statistically derived values, omission of data in one method can result in unjustifiable differences and conclusions.

MFPD measured by GLD porometry consistently yielded lower values than the nominal size, as shown in Fig. 6. However, in the case of three of the samples, the results for MFPD were within ±10 % of the nominal pore size (15 µm for Asada 16; 41 µm for Asada 45 and 56 µm for Asada 55). In the case of two samples, BPPD, in turn, was within ±10 % of the nominal pore size (16 µm for Asada 16 and 35 µm for Asada 34). The same applied to APD (14.6 µm for Asada 16 and 11.9 µm for Gilson 15.8). In conclusion, MFPD yields results most similar to the nominal pore sizes, compared to BPPD and APD.

According to Fig. 6, the BPPDs measured with the PMI equipment were underestimated for all the Gilson samples. According to Gupta (2010), when a viscous wetting liquid like Silwick is used in the measurements, this liquid layer is left on the pore wall, reducing the pore diameter. However, in the case of Asada samples, the BPPDs were not underestimated. The possible reasons for such results might be in their porous structure. As can be seen from microscopic images in Fig. 1 and confirmed by results in Table 3, the open area in Asada samples was the largest, i.e., it was much easier for the porometer to discharge the wetting liquid from such open samples. The wetting liquid did not linger on the solid surfaces of the porous material in these samples. In contrast, the distance between the pores in the Gilson samples was larger. The excess liquid retained on such surfaces could gradually refill the pores in the sample (Gupta, 2010), which, in turn, kept the tiny layer of Silwick inside the pores in the Gilson sample. An hourglass shape of pores in the electroformed sieves probably promoted such leakage. Therefore, the BPPDs in such pieces were underestimated.

Nevertheless, comparable results were obtained for the BPPD of the porometer, the D100 of the PoreSizer, and the D99.5 of the cut point test. The values were within 2.1 – 4.7 µm for several samples (Asada16, Asada45, Gilson15.8, and Gilson 25.5). The three parameters (the BPPD, D100, and D99.5) describe the same pore characteristic, i.e., the largest pore in a sample, and thus the finding is excellent. The same was found for the MFPD of the porometer, the D50 of the PoreSizer^{TM}, and the Cut Point test. The values were all within 3.4 µm for Asada16, Asada 45, and Gilson15.8.

The results obtained with image analysis using the PoreSizerTM and the Cut point test yielded results differing only marginally from the nominal pore size. The PoreSizerTM (D97) results were within ±4 % of the nominal pore size, and the Cut point test (D97) within ±9 %.

4.5. The capillary constant and its effect on the pore diameter measured by porometry

The value of the capillary constant was calculated for the different wetting liquids using equation (7). The obtained values were 0.00385 m for reverse osmosis water, 0.00134 m for Galwick, and 0.00209 m for Silwick. According to the definition, the pores, whose size is equal to these capillary constants can be considered as capillaries. In other words, the studied liquids could form a meniscus in the capillaries of these particular and lower sizes. As mentioned in the Introduction earlier, Kashin et al. (2011) stated that equation 7 was scientifically incorrect. The authors mentioned that applying the maximum values of the capillary constant obtained by equation 7 to the analytical expressions was improper. The application of equation (8) is not without difficulties either. The samples of this study have plenty of pores whose length ranges from tens to hundreds

of micrometers. The measurement of the volume of liquid in each pore in the samples is impossible.

Table 5   Application of a capillary constant to the calculation of the bubble point pore diameter and the mean flow pore diameter measured with Silwick and Galwick wetting liquids.

Sample	Nominal pore size, [µm]	Silwick				Galwick			
		BPPD [µm]	BPPD x0.715, [µm]	MFPD [µm]	MFPD x0.715, [µm]	BPPD [µm]	BPPD x0.715, [µm]	MFPD [µm]	MFPD x0.715, [µm]
Asada 16	16.0	16	11.4	14.7	10.5	18.7	13.4	18	12.9
Asada 34	34.0	34.8	24.9	30	21.5	38.5	27.5	35.4	25.3
Asada 45	45.0	53.1	38	41	29.3	58.8	42	52.7	37.7
Asada 55	55.0	65.7	47	55.7	39.8	95.8	68.5	72.7	52
Gilson 15.8	15.8	12.2	8.7	12	8.6	12.4	8.9	11.6	8.3
Gilson 20.7	20.7	18.3	13.1	17.1	12.2	18.9	13.5	18.6	13.3
Gilson 25.5	25.5	21.7	15.5	19.8	14.2	23.3	16.7	22.9	16.4

The use of 0.715 as the capillary constant, *B*, in equation 3 reduced the pore diameter value, as can be seen from Table 5 and Fig. 7. As can be seen from the data, using the capillary constant *B* to adjust the MFPD was not necessary. Without the adjustment with 0.715, the MFPDs obtained and calculated by the software of the porometer using Silwick as the wetting liquids were very similar to the nominal pore sizes and the D50 measured by the other two techniques studied in this paper. The use of the constant 0.715 led to the underestimation of the MFPD when comparing it with the nominal pore size. When Silwick was used as the wetting liquid, 0.715 reduced the already slightly underestimated MFPD by almost 30 %. Here, the nominal pore diameter of Gilson 15.8 was 15.8 µm, the MFPD was 12 µm, and the one adjusted with the capillary constant was 8.6 µm. The same

trend was observed for the results measured with Galwick. The use of a capillary constant, in this case, underestimated the already low results obtained with this fluid. Using Silwick, the results were already very similar to the nominal pore size and to the D100 and D99.5 without adjusting the capillary constant. The adjustment of the results was not required. In general, applying 0.715 to adjust the results obtained with the porometer, as suggested in the standard ASTM F316, was not reasonable nor necessary for the samples studied in this work. However, this conclusion can be based on the assumption that the tortuosity in these studied samples was very low. For more complex structures (woven multifilament fabrics, ceramics, etc.), the situation could be totally different. Therefore, the use of the capillary constants to these complex structures requires additional research.
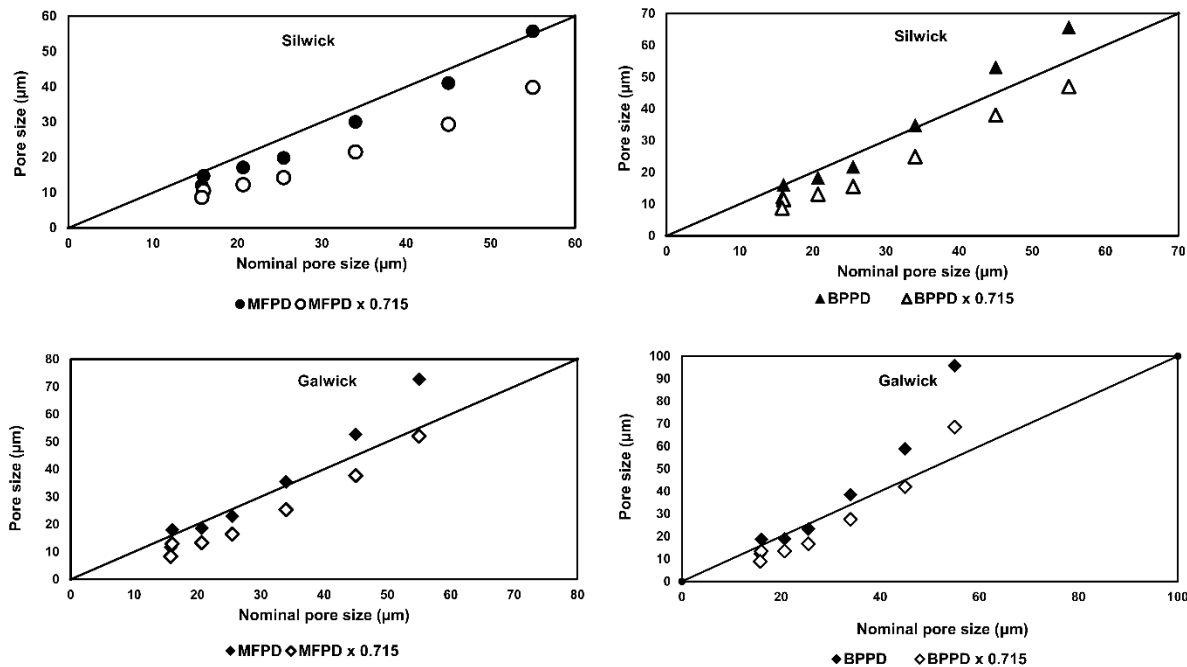

Fig. 7 The comparison of the MFPD (for Silwick and Galwick wetting liquids) and BPPD measured by the capillary flow porometry and with the application of a factor B equal to 0.715.

36

5. Conclusions

Gas-liquid displacement porometry is a technique used to measure different pore characteristics, such as the bubble point pore diameter, the mean flow pore diameter, and the pore size distribution. The technique does not require toxic substances for testing, does not damage the sample, and has many advantages. However, researchers often criticize the quality of the results obtained by GLD porometry. This work aimed to evaluate the validity of the results obtained using GLD porometry. The evaluation was done by comparing the results with those obtained using other methods: image analysis by PoreSizer^{TM} and the Cut point test. Particular attention was also paid to the influence of the capillary constant, which is included in the calculation routine used in GLD porometry described by the ASTM F316 standard.

The results show that GLD porometry should be performed using Silwick as the wetting liquid to obtain comparable results with other techniques. The results obtained with this wetting liquid were close to the nominal pore sizes provided by the cloth manufacturers. This wetting liquid was the only one that could completely wet the studied samples made of nickel and stainless steel. Comparable results were obtained between the BPPD from GLD porometry, the D100 from image analysis, and the D99.5 from the Cut point test. The use of MFPD provided similar results with D50 measured by both image analysis and the cut point test. The PoreSizer^{TM} and the Cut point test, in turn, provide very similar results with the nominal pore size indicating good alignment of all the studied techniques.

The ASTM F316 standard describing the calculation routine used in GLD porometry includes a capillary constant. However, the justification for such a parameter for calculations and its actual physical meaning is unclear or not even addressed in the standard. Analysis of existing literature

shows that the capillary constant has various meanings. At least five different approaches can be found, with all of them not applicable in calculating pore diameter in GLD porometry (due to discrepancies in dimensional analysis, for example). In this study, it became evident that the somewhat arbitrary factor 0.715, claimed to be a capillary constant, to calculate the pore diameter was in no way necessary and even yielded more erroneous results in the case of simply structured filter media. However, the situation can be completely different in the case of materials with complex structures, such as woven multifilament fabrics, double-layer fabrics, ceramics, etc. The use of the capillary constant in calculating the pore diameter in these complex structures requires further research.

ACKNOWLEDGEMENTS

AUTHOR CONTRIBUTIONS

Conceptualization, Methodology, Writing- Original draft preparation, Investigation [M. Ängeslevä]; Resources [G. Rideal]; Writing - Review & Editing, Supervision [R. Salmimies, A. Häkkinen].

Statements and Declarations

The authors declare that they have no known competing financial interests or personal relationships that could have appeared to influence the work reported in this paper.

Data availability

All data generated or analysed during this study are included in this published article. All tables and figures are the author's original work, and no permissions are required.

REFERENCES

AlMarzooqi, F.A., Bilad, M.R., Mansoor, B., Arafat, H.A., A comparative study of image analysis and porometry techniques for characterization of porous membranes, *J. Mater Sci,* 51, pp. 2017 – 2032, 2016, DOI:10.1007/s10853-015-9512-0

Al-hadidi, A.M.M., Limitations, improvements, alternatives for the silt density index, PhD diss., The University of Twente, The Netherlands, 2011, DOI: 10.3990/1.9789036531573

Anlauf, H., The "true" pore size of textile filter media and its relevance for the filtration process with respect to the interaction with apparatus and suspension, *Filtech*, Cologne, Germany, 2016.

ASTM F316-03: 2011, Standard test methods for pore size characteristics of membrane filters by bubble point and mean flow pore test.

Bechhold, H., Durchlässigkeit von Ultrafiltern, Zeitschr. Physik Chemie, 64, pp. 328 – 342, 1908, DOI:10.1515/zpch-1908-6420

Belov, S.V., *Permeable Porous Materials*, Metallurgy Pub., Moscow, 1987.

CFP-1500AEXCS, PMI Capillary Flow Porometer 7.0, User manual, v.6.71.122, Porous Materials, Inc., Ithaca, NY, 2009.

Christov, N.C., Danov, K.D., Kralchevsky, P.A., Ananthapadmanabhan, K.P., Lips, A., Maximum bubble pressure method: universal surface age and transport mechanisms in surfactant solutions, *Langmuir*, vol. **22**, 18, pp. 7528 – 7542, 2006, DOI:10.1021/la061239h

Frolov, Y.G., *Course of colloid chemistry. Surface phenomena and dispersed systems*, Textbook for high schools, 2nd ed., Chemistry, Moscow, 1988.

Green, S.I., Wang, Z., Waung, T., Vakil, A., Simulation of the flow through woven fabrics, *Comput. Fluids*, 37, pp. 1148 – 1156, 2008, DOI: 10.1016/j.compfluid.2007.10.013

Gupta, K., *Porous materials and their pore structure,* Porous Materials, Inc., Ithaca, NY, 2010.

Hernandez, A., Calvo, J.I., Pradanos, P., Tejerina, F., Pore size distributions in microporous membranes. A critical analysis of the bubble point extended method, *J. Membr. Sci*., vol. **112**, 1, pp. 1 – 12, 1996, DOI:10.1016/0376-7388(95)00025-9

Herper, D., Enhancing bubble point testing capabilities on wire meshes by numerical analysis, *F&S International Edition for Filt. Sep.*, 17, pp. 35 – 38, 2017.

Hutten, I. M., *Handbook of nonwoven filter media*, 2nd ed., Butterworth-Heinemann Pub., UK, 2016.

Islam, Md. A., Hossain, M. S., Garcia-Payo, C., Khayet, M. & Ulbricht, M. Mixed Poiseuille-Knudsen flow model for gas liquid displacement porometry data treatment. *J. Membr. Sci.*, 612, 118422, 2020. DOI:10.1016/j.memsci.2020.118422

Jena, A., Gupta, K., Advances in pore structure evaluation by porometry, *Chem. Eng. Techol.*, vol. **33**, 8, pp. 1241 – 1250, 2010. DOI:10.1002/ceat.201000119

Jin, Y., Misra, S., Homan, D., Rasmus, J., Effect of wettability of conductive particles on the multifrequency conductivity and permittivity of fluid-filled porous material, *Fuel*, 268, 2020, 117411, DOI:10.1016/j.fuel.2020.117411.

Kashin, V.V., Shakirov, K.M., Poshevneva, A.I., The capillary constant in calculating the surface tension of liquids, *Steel Transl.*, vol. **41**, 10, pp. 795 – 798, 2011, DOI:10.3103/S0967091211100093

Kikoin, A.K., Kikoin, I.K., *General course of physics. Molecular physics*, 2nd ed., Science Pub., Moscow, 1976.

Kolb, H.E., Schmitt, R., Dittler, A., Kasper, G., On the accuracy of capillary flow porometry for fibrous filter media, *Sep. Purif. Technol.*, vol. **199**, pp. 198 – 205, 2018, DOI:10.1016/j.seppur.2018.01.024

Labuntcov, D.A., Yagov, V.V., *The mechanics of two-phase systems*, 2nd ed., MEI Pub., Moscow, 2007.

Maalal, O., Prat, M., Peinador, R. & Lasseux, D. Determination of the throat size distribution of a porous medium as an inverse optimization problem combining pore network modeling and genetic and hill climbing algorithms, *Phys. Rev. E*, 103, 023303, 2021a, DOI: 10.1103/PhysRevE.103.023303

Maalal, O., Prat, M., Peinador, R. & Lasseux, D. 2021b Identification of local contact angle distribution inside a porous medium from an inverse optimization procedure, *Phys. Rev. Fluids*, 6 (10), 104307, DOI: 10.1103/PhysRevFluids.6.104307

Maalal, O., Prat, M., Peinador, R. & Lasseux, D. Evaluation of pore size distribution via fluid-fluid displacement porosimetry: the viscous bias, *Int. J. Multiph. Flow*, vol. **149**, 103983, 2022, DOI: 10.1016/j.ijmultiphaseflow.2022.103983

Miller, R., Fainerman V.B. Chapter 6 - Surfactant adsorption layers at liquid-fluid interfaces, *Handbook of Surfaces and Interfaces of Materials*, vol. 1, 2001, pp. 383-421.

Morison, K. R. A comparison of liquid-liquid porosimetry equations for evaluation of pore size distribution, *J. Membr. Sci.*, 325, pp. 301 – 310, 2008, DOI:10.1016/j.memsci.2008.07.042

Mourhatch, R., Tsotsis, T. T. & Sahimi, M. Determination of the true pore size distribution by ow permporometry experiments: An invasion percolation model. *J. Membr. Sci.*, 367, pp. 55 – 62, 2011, DOI: 10.1016/j.memsci.2010.10.042

Mayer, V. V., *Drops. Jets. Sound, Educational Studies*, PhysMathLit, Moscow, 2008.

Purchas, B.D., Sutherland, K., *Handbook of filter media*, Elsevier Science Ltd., UK, Oxford, 2002.

Richards, T.W., Carver, E.K., A critical study of the capillary rise method of determining surface tension, with data for water, benzene, toluene, chloroform, carbon tetrachloride, ether and dimethyl aniline, *J. Am. Chem. Soc.*, vol. **43**, 4, pp. 827 – 847, 1921, DOI: 10.1021/ja01437a012

Rideal, G., Stewart, A., Challenge testing: Part 1 – wet testing – investigating the measurement uncertainties associated with different definitions of maximum pore size, *Filtr.*, vol. **17**, 2, pp. 100 – 102, 2017.

Rushton, A., Ward, A., Holdich, G. R. *Solid-liquid filtration and separation technology*, 2nd ed., Wiley-VCH Verlag GmbH, Weinheim, Germany, 2000.

Salmimies, Acidic dissolution of iron oxides and regeneration of a ceramic filter medium, PhD, Acta Universitatis Lappeenrantaensis 495, 2012.

Salmimies, R., Kallas, J., Ekberg, B., Häkkinen, A., Oxalic acid regeneration of ceramic filter medium used in the dewatering of iron ore, *ISRN Chem. Engin.*, 2012, pp. 1 – 6, vol **2012**, DOI: 10.5402/2012/921873

Savitskaya, T.A., Shimanovich, M.P., *Practical work on colloid chemistry. Part 1 "Surface Phenomena",* BSU, Minsk, 2003.

Scheidegger, A. E., *The physics of flow through porous media*, University of Toronto Press, 1963.

Siau, J. F., Kanagawa, Y., Petty, J.A., The use of permeability and capillary theory to characterize the structure of wood and membrane filters, *Wood and Fiber*, vol. **13**, 1, pp. 2 – 12, 1981.

Yu, J., Hu, X., Huang, Y., A modification of the bubble-point method to determine the pore-mouth size distribution of porous materials, *Sep. Purif. Technol.*, vol. **70**, 3, pp. 314 – 319, 2010, DOI:10.1016/j.seppur.2009.10.013

Vallabh, P., Banks-Lee, P., Seyam, A.-F. New approach for determining tortuosity in fibrous porous media. *J. Eng. Fiber. Fabr.*, 5, pp. 7-15, 2010, DOI: 10.1177/155892501000500302

Zhang, H., Araya, K., Guo, G., Ohmiya, K., Capillary zone from a watertable, *Eng. Agric. Environ. Food*, vol. **3**, 3, pp. 72 – 78, 2010, DOI: 10.1016/S1881-8366(10)80011-4

Zhang, P., Ni, B., Research of influence of wetting fluid by gas bubble method to measure pore size characteristics, *Adv. Mat. Res.*, 1048, pp. 498 – 502, 2014, DOI: 10.4028/www.scientific.net/AMR.1048.498